
K.Sh. Kakhramanov, F.K. Aleskerov, S.Sh. Kakhramanov, S.A. Nasibova

Scientific and Production Association “Selen”, National Academy of Sciences of Azerbaijan,
29 A, G. Dzavida Ave., Baku, AZ 1118, Azerbaijan

**SELF-ORGANIZATION OF LOW-DIMENSIONAL NANOSTRUCTURES
IN LAYERED CRYSTALS OF $A_2^{V}B_3^{VI}$ TYPE**

Materials with nanoisland arrays, corrugated and stepped structures-nanowires of different size and density have been obtained. A mechanism of formation of the above nanostructures has been described, which is due to migration, coalescence and clustering of nanoislands in the interlayer space of undissolved impurity and superstoichiometric excess, as well as due to plastic deformation effect under a pressure of thermal wave forming corrugated structures. Single-dimensional charge flow channels have been discovered, the percolation character of charge carrier transport in the network with respective quantum dot distribution density has been determined. The thermoelectric performance of nanostructured crystals has been improved.

Key words: nanowires, clustering, nanoislands, deformation, corrugated structures, single-dimensional channels, percolation.

Introduction

Figure of merit improvement of thermoelectric materials by reducing the phonon component of thermal conductivity, as well as by increasing the Seebeck coefficient through density of states increase near the Fermi level is the subject of much investigation today. One of the ways to accomplish this purpose is reducing dimensions of thermoelectric component parts, namely using quantum dots and wires for efficient phonon scattering on the edges of these nanostructures, and using specific distribution in the density of states. The size and shape, and well as the composition of nanostructures markedly affect the electrophysical characteristics of material, and one must select optimal for thermoelectricity parameters which is associated with process design of materials with given properties. For instance, quantum dots, self-organizing in the interlayer space, efficiently scatter and restrict the propagation of phonon modes, but, at the same time, transport which is partially transformed to hopping type reduces charge carrier mobility. Therefore, it is necessary to select a mode with restricted phonon propagation and simultaneous efficient charge transport. In order to solve these problems, we employed nanostructured material technology using self-organization effects of low-dimensional nanostructures by growing crystals under different rate, annealing and thermal fluctuation conditions, as well as thermal diffusion intercalation.

To increase as much as possible the thermoelectric figure of merit of materials, the electron conductivity should be possible higher with the lowest thermal conductivity. The thermoelectric properties can be improved by using space inhomogeneous materials whose inhomogeneities are comparable in size to characteristic wavelengths of electrons (10 – 50 nm) or phonons (1 nm), i.e. lie in nanometer region. Thermal conductivity can be reduced considerably by thermal flux scattering on interfaces, and conditions should be selected so that interface could scatter phonons, rather than electrons. Description and calculation of the model of such quantum tunnelling transport is given in [1, 2].

Crystals were prepared by vertical directional crystallization method at a temperature gradient

$\Delta T = 100$ degrees/cm and crystallization rate 1; 2 and 2.5 cm/hour. AFM (atomic force microscope) images were obtained using Solver Next scanning probe microscope. X-ray diffractometer investigations of (0001) surface were performed on Philips Panalytical X'Pert Pro XRD diffractometer.

Nanoislands, nanowires, nanosteps and corrugated structures, dislocation centres play a decisive quantum-mechanical role in the localization and transfer of charge and heat. The choice of such high-performance substances should be based on the knowledge of structure-property interaction for $A_2^{VII}B_3^{VI}$ compounds and their solid solutions with interlayer strictly oriented nanoparticles. Formation of these structures is due to mass transfer and plastic deformation whose nature and regularities are inherent in organization of similar structures in other solid-state materials.

As is known, in many layered crystals there is the effect of stoichiometric excess and impurity ejection from the layers that form crystal blocks to the interlayer van der Waals space. Such self-purification is called self-intercalation effect [3]. With certain impurities, this process can be accompanied by a change in electrical activity. Self-organization of nanostructures on the surface of interlayer space leads to formation of elements depending in their form on the composition and amount of impurity and the temperature conditions of diffusion and annealing. In this context, of interest are layered systems whose van der Waals spaces can serve as nanoreactors [4, 5, 6] for the formation of various nanofragments. Alignment of impurity clusters into quantum dot array on (0001) surface of crystal is interesting in terms of material properties control.

Discussion of the results

Supposed diffusion paths and their aggregation are related to the process of filling with impurities of places around the dislocation networks and vacant sites, such as telluride (selenium) vacancies on the van der Waals (0001) surface (Fig. 1). Due to active interaction in annealing, impurities are formed around these dislocation networks to form nanoobjects (Fig. 2), including interlayer nanostructured elements (INSE). Diffusion processes in the line of basal (0001) surface not only form individual nanostructured elements, but also connect them by a continuous chain, forming charge percolation channels along the direction of crystal growth.

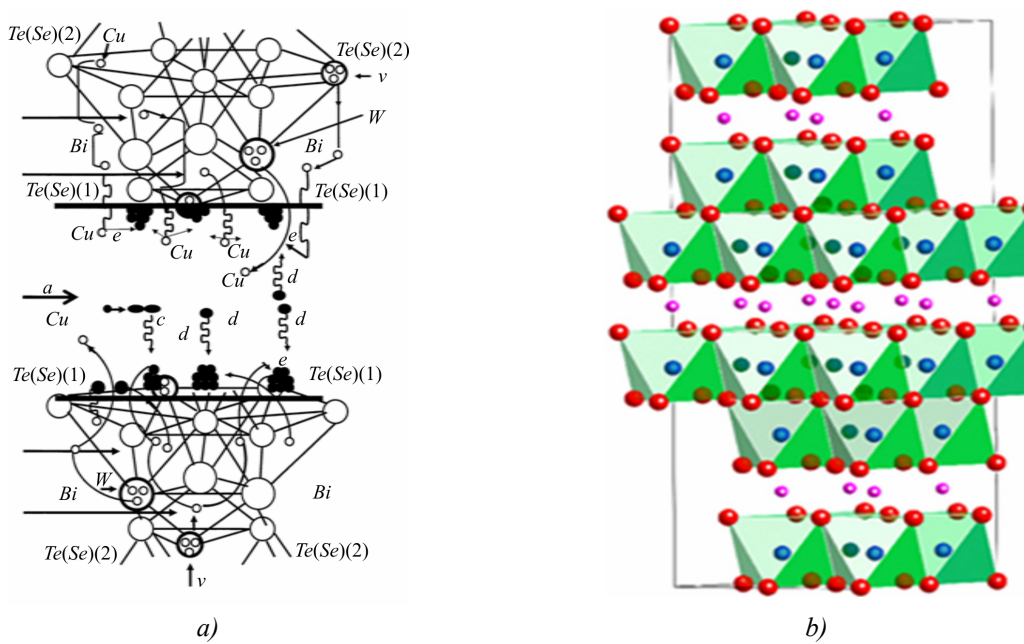
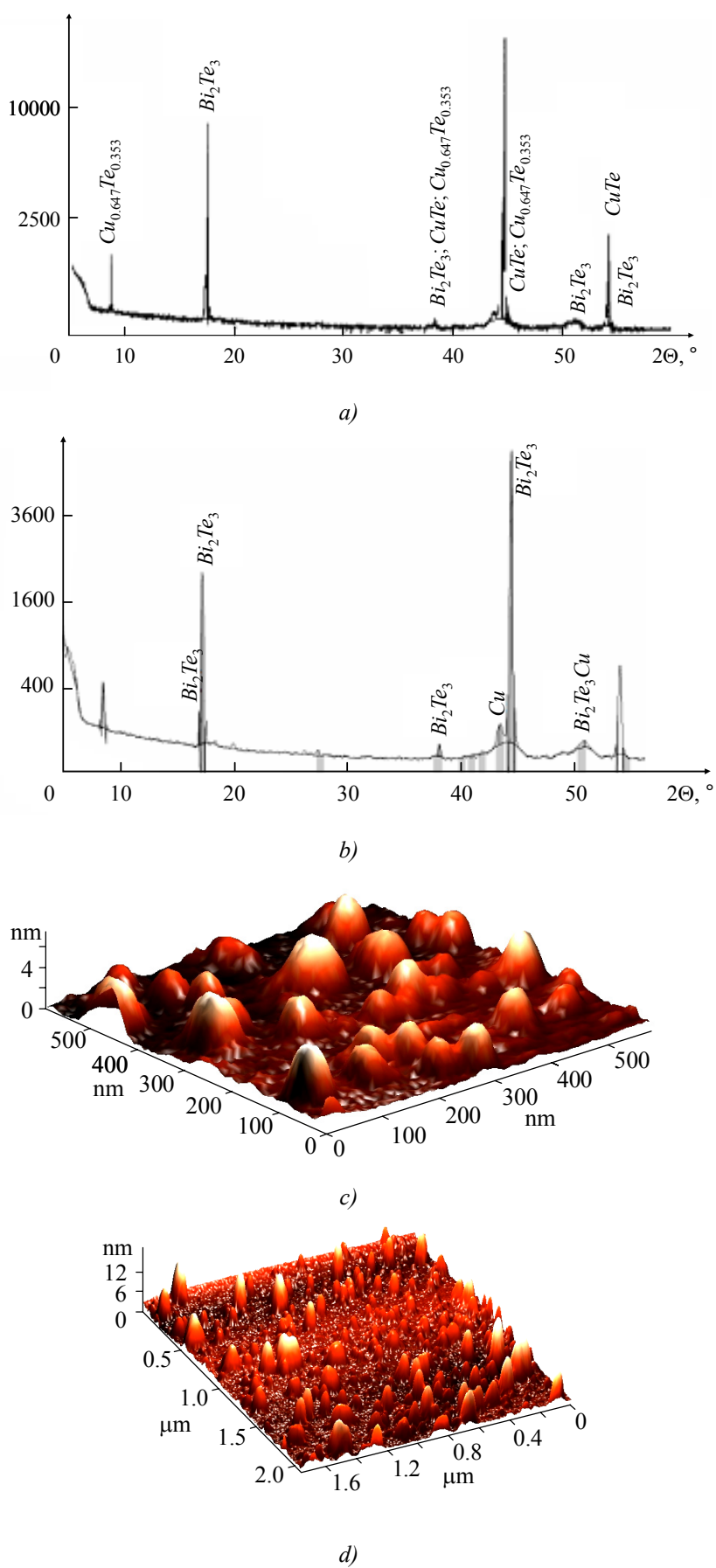


Fig. 1. Schematic of INSE aggregation paths in Bi_2Te_3 doped (a) and intercalated (b) with copper.



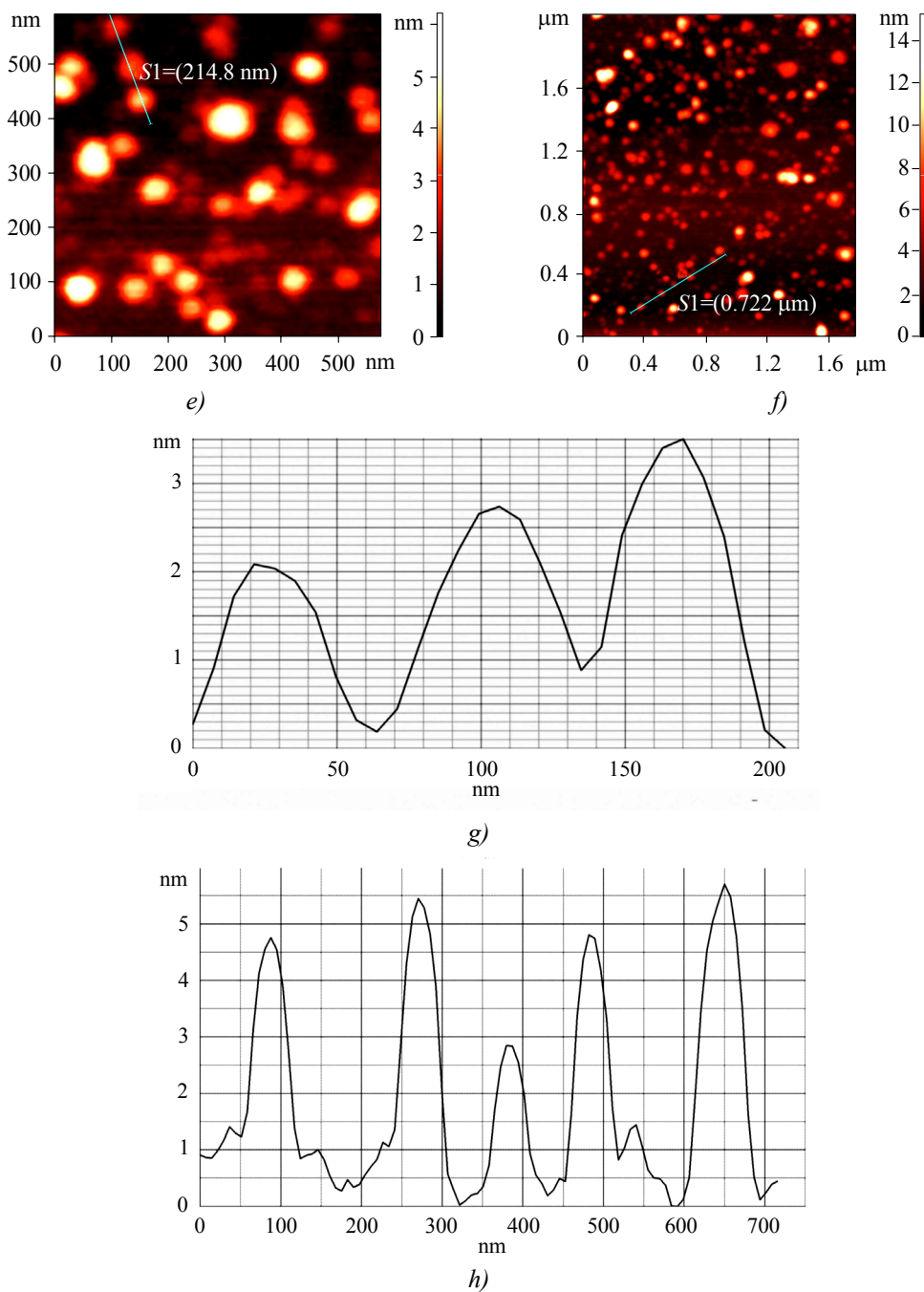


Fig. 2. X-ray diffractogram of copper doped Bi_2Te_3 – a); X-ray diffractogram of copper intercalated Bi_2Te_3 – b);
 3D AFM image of $Bi_2Te_3 < Cu >$ – c); 3D AFM image of copper intercalated Bi_2Te_3 – d);
 2D AFM image of $Bi_2Te_3 < Cu >$ – e); profilogram of doped $Bi_2Te_3 < Cu >$ – f);
 2D AFM image of copper intercalated Bi_2Te_3 – g); profilogram of copper intercalated Bi_2Te_3 – h).

These structures by definition are quantum dot superlattices.

Quantum dots (nanoislands) and their distribution density should be considered as one of the factors determining percolation threshold on the lattice in (0001) $A_2^{V}B_3^{VI}$ <impurity> plane [7, 8]. In $Te^{(1)}-Te^{(1)}$ layer on the van der Waals surface having the greatest “gap” there are nanoisland arrays – some analogy of quantum dots. In this way infinitely connected structures are formed consisting of separate INSE and interconnected by a continuous chain; thus tunnelling current can flow along the conducting channels (bonds) through bonded INSE. With formation of superstructure in Bi_2Te_3 the

temperature dependences of kinetic properties can be of extreme kind [6]. Along the layers between the opposite lattice sides in $Te^{(1)}-Te^{(1)}$ space, charges can be transferred through nanoisland array affecting the general density of electric current. Percolation effect on (0001) Bi_2Te_3 surface which is either of the two sides of $Te^{(1)}-Te^{(1)}$ layers, influence of surface relief on percolation threshold leading to magnetoresistance oscillation and changes in kinetic parameters (Fig. 3) are of certain interest.

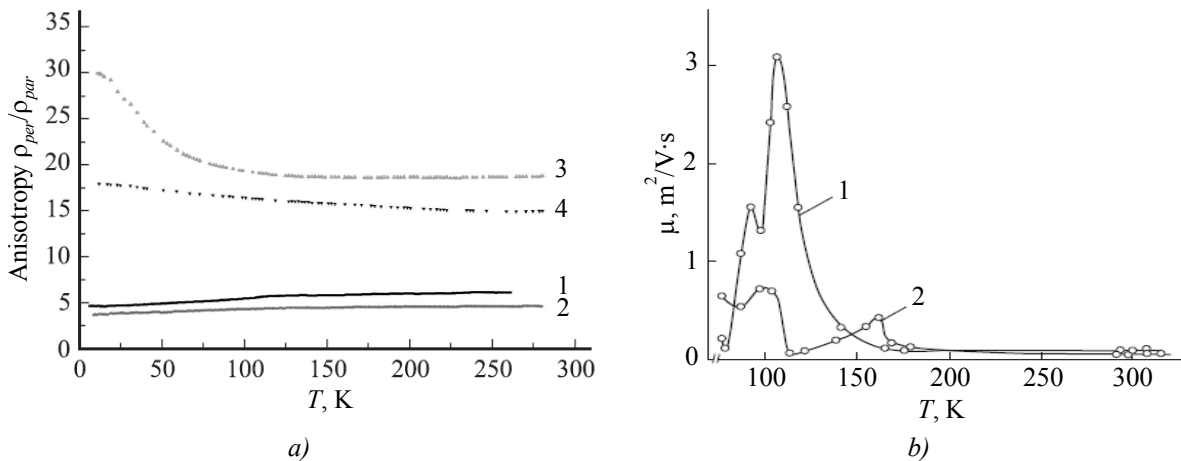


Fig. 3. Temperature dependences of resistivity anisotropy of Bi_2Te_3 single crystals in the temperature range of $5 < T < 300$ K: 1 – undoped Bi_2Te_3 , 2 – $Bi_2Te_3(Cu)$, 3 – $Bi_2Te_3(Cu, In)$, 4 – $Bi_2Te_3(B)$ – a); Temperature dependences of charge carrier mobility of $Bi_2Te_3<Ni, 0.5$ mas.%> at $H \perp c \perp I$ (1) and $H \parallel c \perp I$ (2) – b).

Percolation threshold is determined by the density of nanoislands distribution. The process of INSE aggregation and percolation in $Te^{(1)}-Te^{(1)}$ space is similar to the model of description of percolation cluster assembly on a free lattice (Fig. 4). This model assumes that a particle moving in space and touching a cluster will adhere to it with certain probability. In the simplest arrangement in a two-dimensional $Te^{(1)}-Te^{(1)}$ space it turns out that (0001) surface is considered as a square lattice (cell). Thus, each particle moves to the neighboring square randomly. If a particle reaches the boundary of $Te^{(1)}$, it is either reflected from it, or deposited in telluride vacancies and on dislocation walls. Being aggregated, the particle stops and is fixed in this lattice. Diffusion process, when continued, forms a two-dimensional surface cluster of percolation type, extending along (0001) basal plane. During certain stages INSE grow normal to (0001) plane, which is clearly seen from 3D AFM images (Figs. 5, 7). The process of coagulation in $Te^{(1)}-Te^{(1)}$ space reaches a maximum whereby contacting INSE are united into a single fractal surface above the percolation threshold.

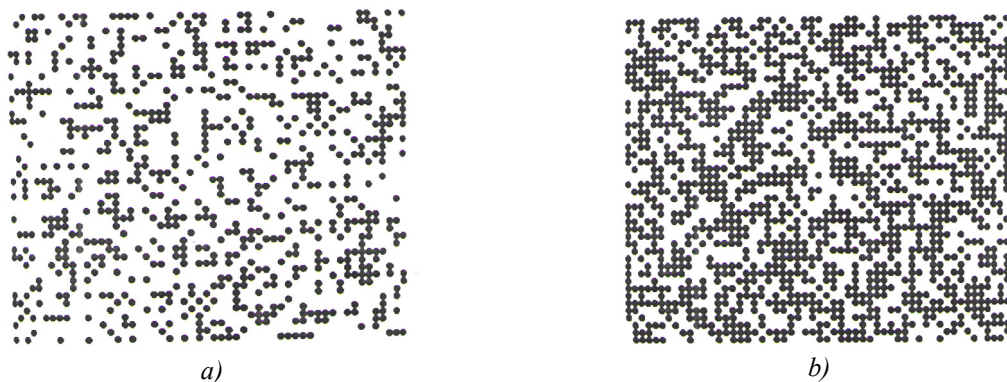


Fig. 4. Simulated square lattices with random sites for comparison to AFM images of the (0001) surface of crystals: a) Square lattice with randomly occupied sites below the percolation threshold; b) Square lattice with site occupancy probability equal to percolation threshold.

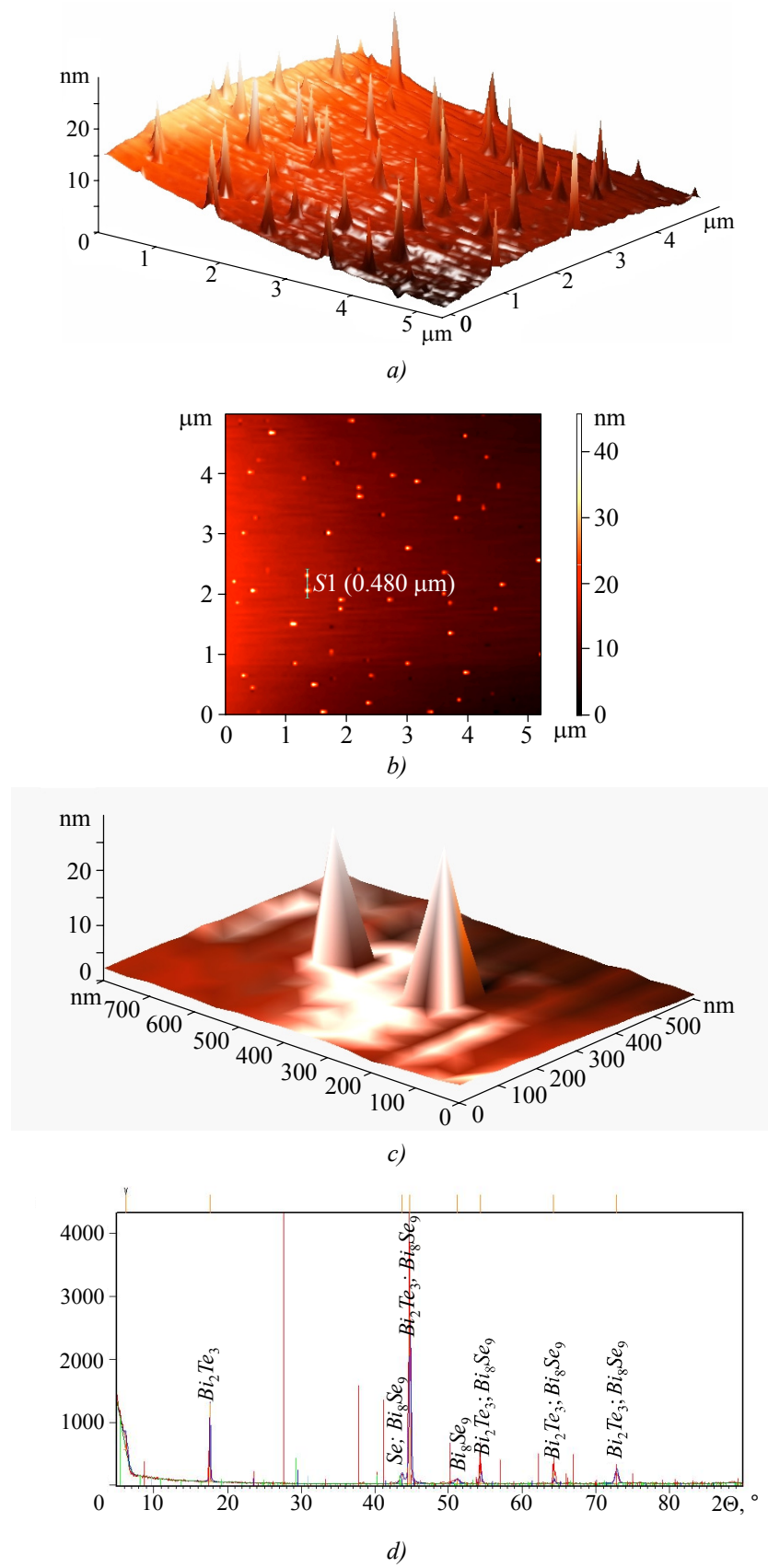
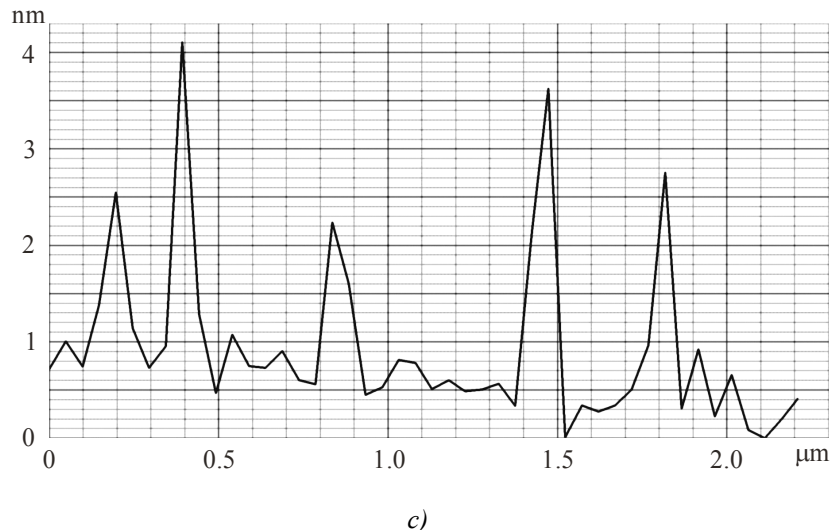
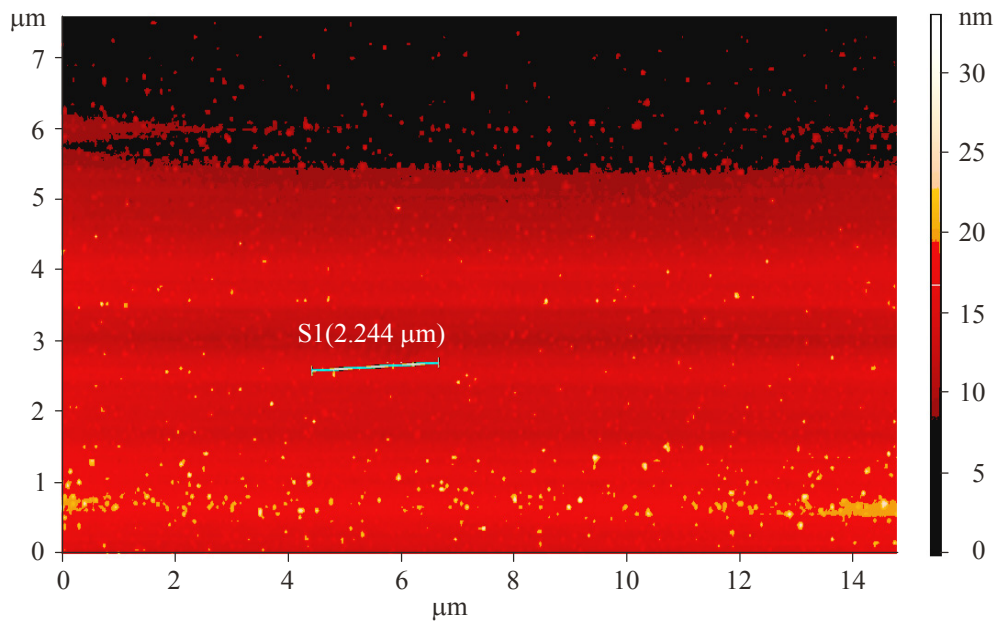
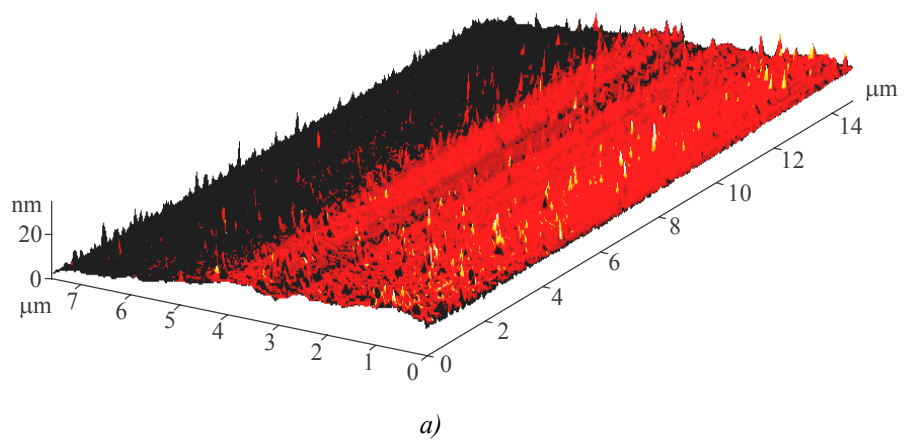
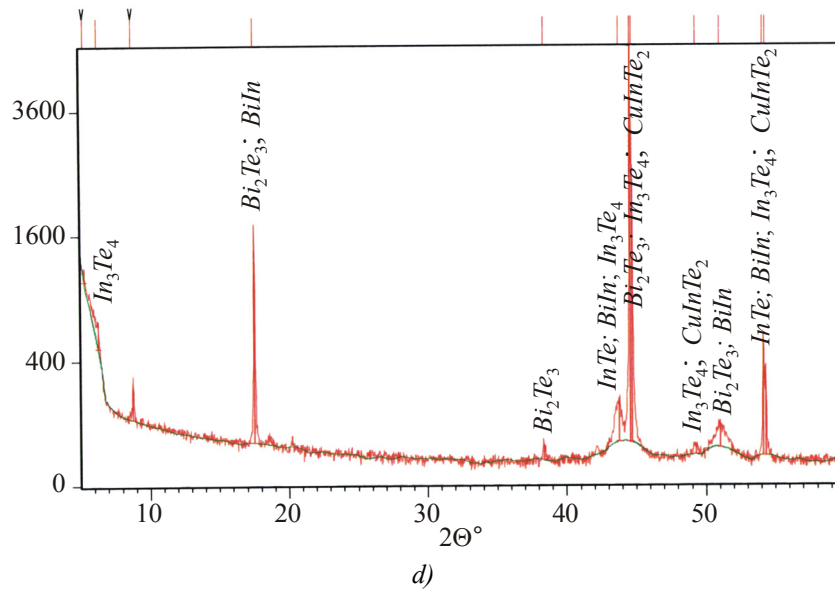
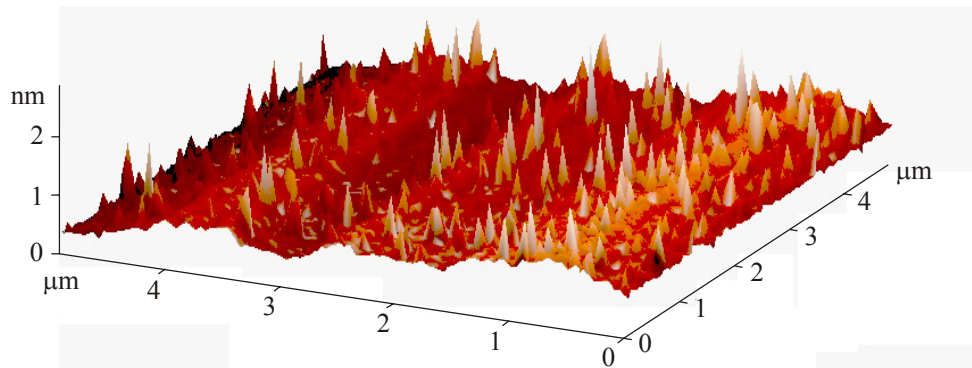


Fig. 5. 3D AFM image of doped $\text{Bi}_2\text{Te}_3\text{Se}$ – a); 2D AFM image of $\text{Bi}_2\text{Te}_3\text{Se}$ – b);
 3D AFM image of a fragment of two nanoislands of $\text{Bi}_2\text{Te}_3\text{Se}$ – c);
 X-ray diffractogram of $\text{Bi}_2\text{Te}_3\text{Se}$ with Se traces at $2\theta = 44^\circ$ – d).

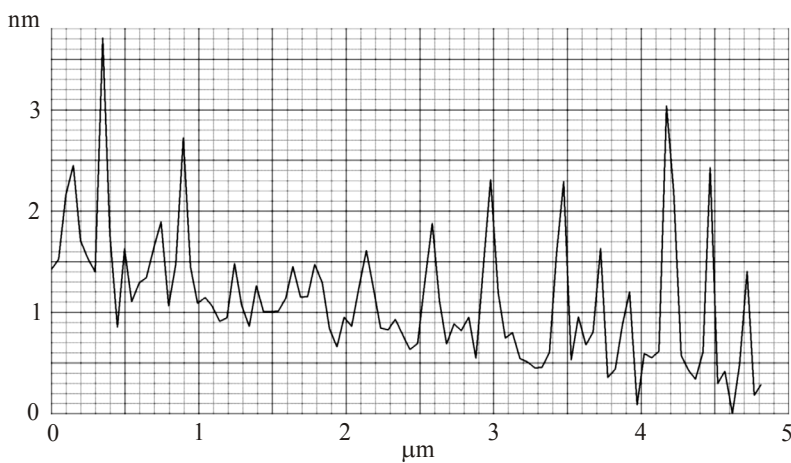




d)



e)



f)

Fig. 6. 3D AFM image in Bi_2Te_3 -In+Cu system – a); 2D AFM image in Bi_2Te_3 -In+Cu system – b); profilogram along the section given in Figs. b), c); X-ray diffractogram of Bi_2Te_3 -In+Cu – d); fragment of 3D AFM image of Bi_2Te_3 -In+Cu – e); profilogram of Bi_2Te_3 -In+Cu fragment – f).

Materials with interlayer nanostructures are quantum dot (QD) superlattices consisting of impurity clusters several nanometers in size. If QD density is above the respective percolation threshold, conductivity in them takes place in single-dimensional channels by diffusional mechanism. Below the percolation threshold nanostructures possess hopping conductivity due to tunnelling of electrons through the barriers dividing QD. Transition from hopping to diffusion transport is observed with a change in QD density and the degree of their filling with charge carriers.

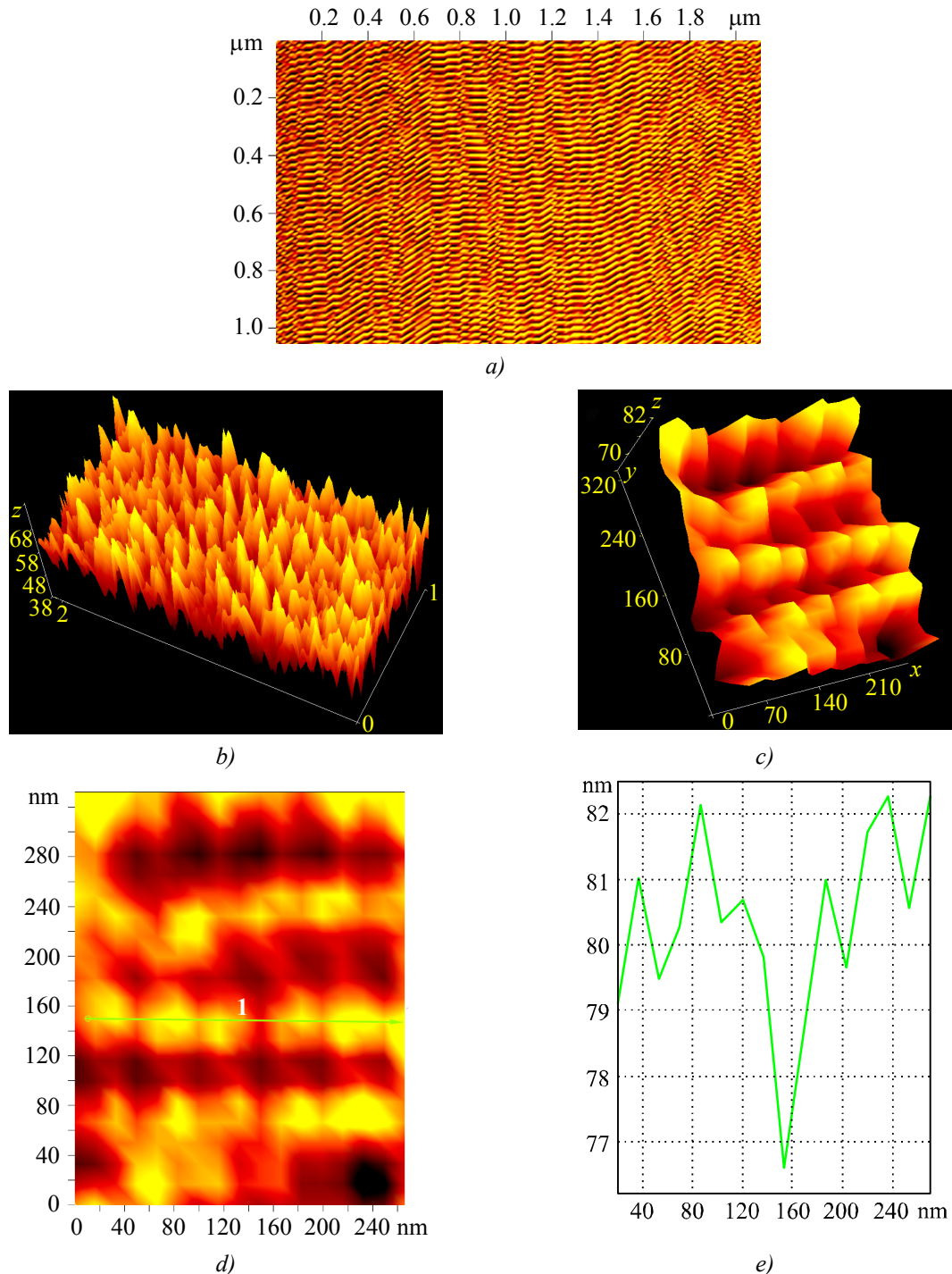


Fig. 7. 2D AFM image of $Bi_2Te_3<Ag>$ – a); 3D AFM image of $Bi_2Te_3<Ag>$ – b);
 3D AFM image of $Bi_2Te_3<Ag>$ – c); fragment of 2D image of $Bi_2Te_3<Ag>$ – d);
 profilogram along the (1)line (see Fig. d) – e).

The main reason for stressed islands formation on the surface is relaxation of elastic stresses on the edges of layers and interaction of islands through stresses they create in the crystal. The shape of QD can vary considerably in the course of healing or postgrowth annealing. Fig. 8 demonstrates the final result of the dynamics of large islands formation from small ones and linear formations formed of QD that can be called quantum wires. The aggregated structures interconnected by a continuous chain of clusters assure charge tunnelling in conducting channels.

Electron microscopic images have shown that nanoobjects are formed of nanoislands in diffusion at temperatures above 500 K. Penetrating mainly into the interlayer space, impurities create bulk periodic superstructures consisting of nanoisland arrays between quintet layers which move apart as a result and increase crystal anisotropy. This, in turn, increases the role of “bending” vibrations for crystal thermal properties. The role of this specific branch of acoustic vibrations and its behaviour in layered crystals according to Lifshits theory [9] was reported in [10]. The “bending” branch corresponds to vibrations propagating in layers plane with shifting of atoms in the direction normal to layers and makes the main contribution to heat transfer with the temperature behaviour of three different types. The higher is crystal anisotropy, the more significant is its role in “membrane” effect (growth of “bending” vibration frequency under tension of layers), leading to negative dilatation in layers plane. The anomalies of kinetic parameters that we observed took place in the area of linear temperature growth of heat capacity, with the dominant contribution of “bending” branch. Scattering of this phonon branch at the base of QD that are chemically related to quintets, results in thermalization of QD levels with subsequent tunnelling. This area, where heat capacity $C \sim T^2$, and temperature growth of thermal conductivity coefficient $\chi \sim T^{2+x}$ (where x can be determined by tunnelling processes, i.e. by QD size and density) is observed as the area of thermal anomaly. Note that a drop in lattice thermal conductivity in this area can be somewhat compensated by increased thermal conductivity of tunnelling current. Thermoelectric figure of merit of these samples is 15 % higher than that of undoped ones, probably due to a reduction of total thermal conductivity of “quintet layers-INSE” composite with increased role of phonon scattering on the boundaries of moved apart layers and INSE. These processes are dominated by phonons corresponding to bending vibrations that have a square type of dispersion.

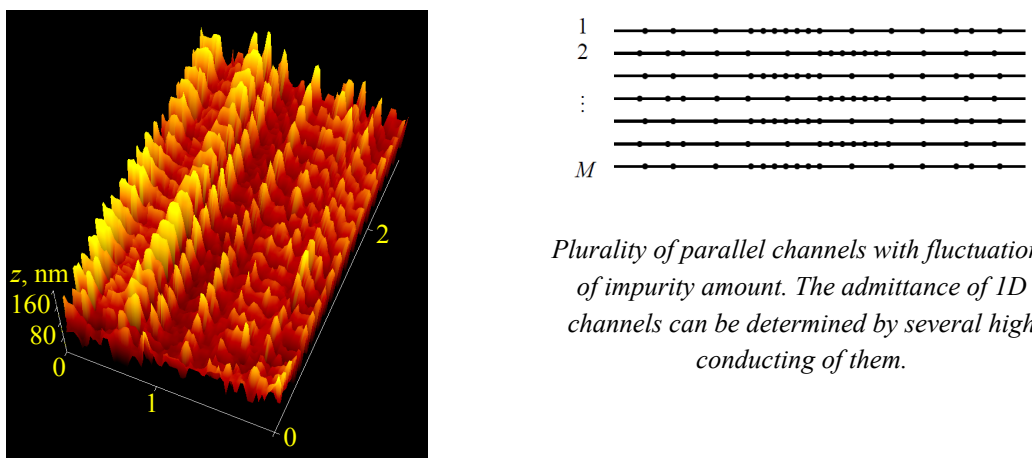


Fig. 8. Ni-doped Bi_2Te_3 : 3D AFM image of $\text{Bi}_2\text{Te}_3<\text{In} + \text{Cu}>$ with parallel conductivity channels.

Plurality of parallel channels with fluctuations of impurity amount. The admittance of 1D channels can be determined by several high conducting of them.

Anharmonic vibrations of structure-forming atoms of layers are one of the factors yielding a relatively uniform linear crystal growth. With increase in elastic stress pressure created by thermal

wave, the linear order of alignment is violated and quintet layers are deformed with a periodic distribution of wrinkles (Fig. 9, 10).

The value of thermal pulse forms an elastic deformation, and when some critical compressive stress is over the limits, quintet layers are aligned in corrugated wavy structures, which attenuates compressive stress. This occurs with increase in the rate of crystal growth by a factor of 2 and 2.5. The wavelength of wrinkles is determined by elastic characteristics and the thickness of quintet layers. The method of calculation of deformed layer thickness versus the wave period [11] can help to determine the number of quintet layers in a corrugated structure. A change in the average “wavelength” λ corresponding to the wrinkles was described by a simple power dependence $\lambda(x) \sim x^m$. The investigated materials differed in the value m . In order to describe their properties correctly, physicists introduced a concept of wrinklon, i.e. structural element whose recurrence characterizes the entire ensemble of wrinkles. A single wrinklon is responsible for a transition area where two wrinkles with the “wavelength” λ are combined to form a larger one. Each wrinklon in this case is matched by certain size L determined by material characteristics and the value of λ .

In this case one can use the expression of the form $\lambda(x)/h \sim (E \cdot h/T)^{0.25} \cdot (x/h)^{0.5}$, where h is layer thickness, E is Young's modulus, and T value characterizes the tensile force.

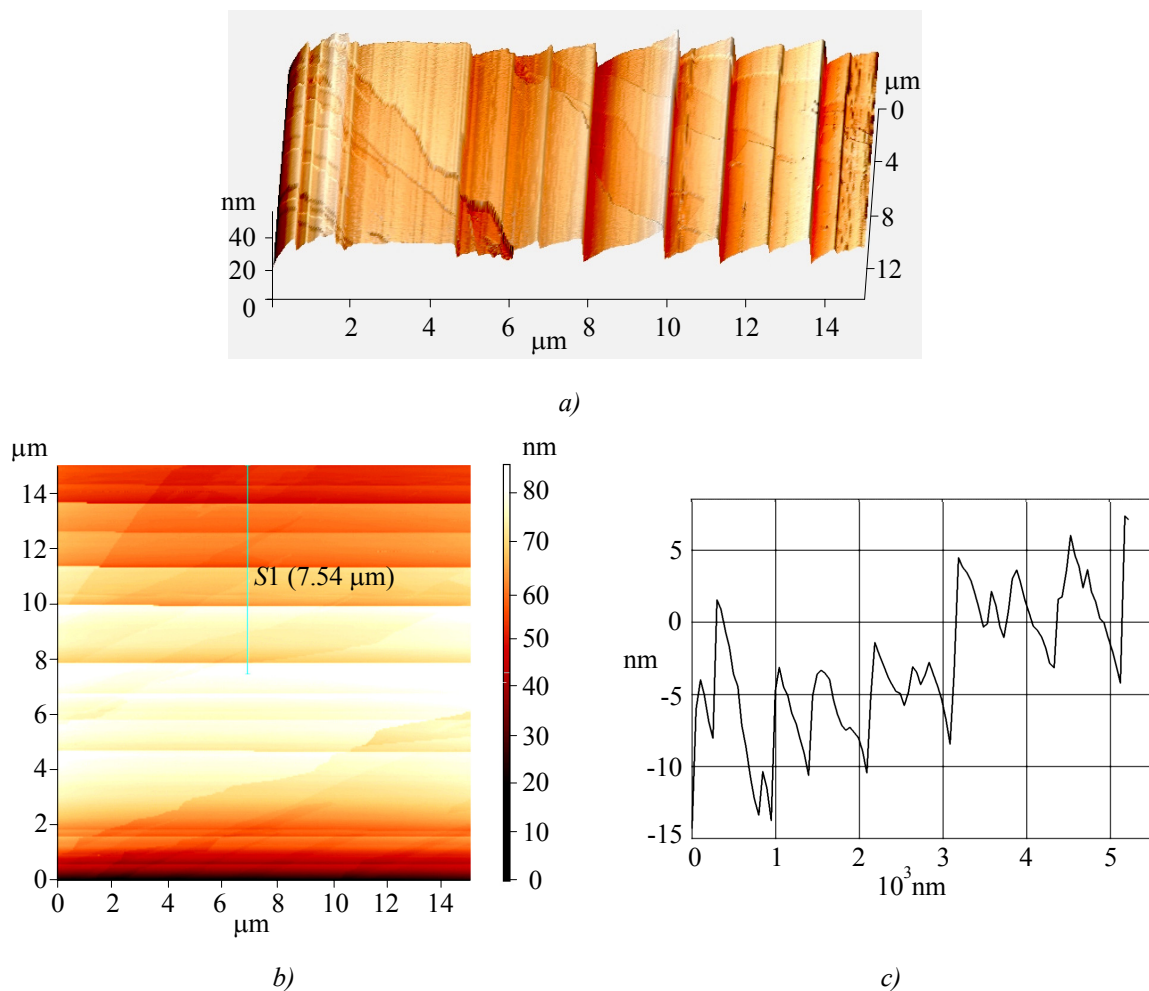


Fig. 9. Corrugated structures $Bi_2Te_3<Ni>$: 3D AFM image of surface – a);
 2D surface – b); cut profilogram in Fig. b) – c).

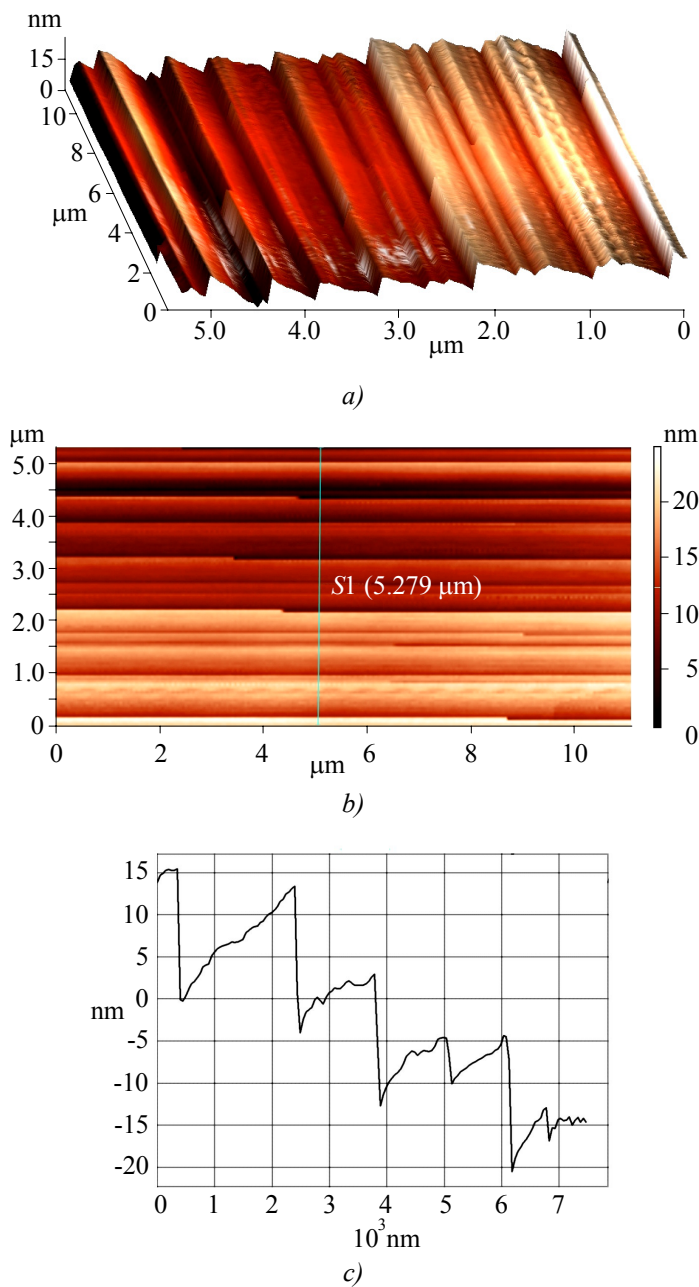


Fig. 10. Corrugated structures $Bi_2Te_3 < Se >$: 3D AFM image of surface – a); 2D surface – b); cut profilogram in Fig. b – c).

Obtaining the right size wrinkles is directly related to crystallization front temperature. Its rise leads to increased viscosity of crystallized area and reduced ability of elastic energy accumulation, owing to which the height of the structure is reduced. Thus, the wavelength of wrinkle and its height correlate in a very small range with crystallization front temperature.

It should be noted that the results obtained are in agreement with the authors' theoretical research [12-14].

Conclusions

Materials with nanoisland arrays, corrugated and stepped structures-nanowires of different size and density have been obtained. A mechanism of formation of the above nanostructures has been

described, which is due to migration, coalescence and clustering of nanoislands in the interlayer space of undissolved impurity and superstoichiometric excess, as well as due to plastic deformation effect under a pressure of thermal wave forming corrugated structures. Single-dimensional charge flow channels have been discovered, the percolation character of charge carrier transport in the network with respective quantum dot distribution density has been determined.

References

1. A.A. Snarskii, A.K. Sarychev, I.V. Bezsdudnov, and A.N. Lagarkov, Thermoelectric Figure of Merit of the Bulk Nanostructured Composites with Distributed Parameters, *Semiconductors* **46** (5), 677 – 683 (2012).
2. L.P. Bulat, D.A. Pshenai-Severin, Effect of Tunneling on the Thermoelectric Figure of Merit of Bulk Nanostructured Materials, *Physics of the Solid State* **52** (3), 452 – 458 (2010).
3. S.Sh. Kakhramanov, Selfintercalation in $Bi_2Te_3 < Cu >$, *Inorganic Materials* **44** (1), 17 – 25 (2008).
4. F.K. Aleskerov, S.Sh. Kakhramanov, Effect of Interlayer Metal Nanofragments on the Kinetic Properties of $Bi_2Te_3 < Cu, Ni >$, *Metallofizika i Noveishie Tekhnologii* **30** (11), 1465 – 1477 (2008).
5. F.K. Aleskerov, S.B. Bagirov, S.Sh. Kakhramanov, and G. Kavei, Thermoelements for Electric Generators Based on Bismuth and Antimony Chalcogenides with Interlayer Nanostructures, *Transactions of Azerbaijan National Academy of Sciences: Series of Physical-Mathematical and Technical Sciences, Physics and Astronomy* **5**, 52 – 55(2010)
6. B.M. Goltsman, V.A. Kudinov, and I.A. Smirnov, *Semiconductor Thermoelectric Materials Based on Bi_2Te_3* (M: Nauka, 1972), 319 p.
7. F.K. Aleskerov, K.Sh. Kakhramanov, and S.Sh. Kakhramanov, Percolation Effect in Bi_2Te_3 Crystals Doped with Copper or Nickel, *Inorganic Materials* **48** (5), 41 – 45 (2012).
8. F.K. Aleskerov, K.Sh. Kakhramanov, and S.Sh. Kakhramanov, Percolation Process in $Bi_2Te_3-In_2Se_3$ System, *Transactions of Azerbaijan National Academy of Sciences: Series of Physical-Mathematical and Technical Sciences, Physics and Astronomy* **2**, 25 – 33 (2010).
9. I.M. Lifshits, On the Thermal Properties of Chain and Layered Structures at Low Temperatures, *JETP* **22** (4), 475 – 486 (1952)
10. N.A. Abdullayev, R.A. Suleymanov, M.A. Aldzhanov, and L.N. Alieva, On the Role of Bending Vibrations in Heat Transfer Processes in Layered Crystals, *Physics of the Solid State* **48** (4), 1775 – 1779 (2002).
11. H. Vandeparre, M. Pineirua, F. Brau, B. Roman, J. Bico, C. Gay, W. Bao, C.N. Lau, P.M. Reis, and P. Damman, Wrinkling Hierarchy in Constrained Thin Sheets from Suspended Graphene to Curtains, *Phys. Rev. Lett.* **106**, 224301 (2011), issue 22 / (arXiv:1012.4325v2 (2010)).
12. K.Sh. Kakhramanov, A.M. Pashayev, B.G. Tagiyev, F.K. Aleskerov, and A.A. Safarzade, Nanostructured Hybrid Structured Based on $A_2^V B_3^{VI} < \text{impurity} >$, *J. Thermoelectricity* **2**, 32 – 41 (2011).
13. E.I. Rogacheva, Percolation Effects and Thermoelectric Material Science, *J. Thermoelectricity* **2**, 61 – 72 (2007).
14. L.P. Bulat, V.T. Bublik, I.A. Drabkin, V.L. Karataev, V.B. Osvensky, G.I. Pivovarov, and D.A. Pshenai-Severin, Bulk Nanostructured Thermoelectrics Based on Bismuth Telluride, *J. Thermoelectricity* **3**, 67 – 72 (2009).

Submitted 20.02.2013.